DIRECT MASS MEASUREMENTS OF EXOTIC NUCLEI IN STORAGE RINGS*

Yu.A. Litvinov[a,b], H. Geissel[b,c], R. Knöbel[b], B. Sun[c,d], H. Xu[e]

[a]Max-Planck-Institut für Kernphysik
Saupfercheckweg 1, 69117 Heidelberg, Germany

[b]GSI Helmholtzzentrum für Schwerionenforschung
Planckstraße 1, 64291 Darmstadt, Germany

[c]Justus-Liebig Universität Giessen
Heinrich-Buff-Ring 16, 35392 Giessen, Germany

[d]School of Physics and Nuclear Energy Engineering, Beihang University
Beijing 100191, China

[e]Institute of Modern Physics, Chinese Academy of Sicences
Lanzhou 730000, China

(Received January 5, 2010)

Mass measurements of exotic nuclei is a fast developing field which is essential for basic nuclear physics and a wide range of applications. The method of storage ring mass spectrometry has many advantages: (1) a large amount of nuclides can be simultaneously measured; (2) very short-lived ($T_{1/2} \gtrsim 50$ μs) and very rare species (yields down to single ions) can be accessed; (3) nuclides in several atomic charge states can be investigated; (4) half-life measurements can be performed with time-resolved mass spectrometry. In this contribution we concentrate on some recent achievements and future perspectives of the storage ring mass spectrometry.

PACS numbers: 21.10.Dr. 29.10.Dh

1. Introduction

Atomic nuclei are many-body systems in which the strong, weak, and electromagnetic fundamental interactions take place by acting between the nucleons. The nuclei are composed of two types of fermions, protons and neutrons, and, therefore, they are natural laboratories to study quantum correlation effects. The net result of all interactions is reflected in the mass of the nucleus (*i.e.* in its binding energy). Nuclear mass surface is a sensitive

* Presented at the XXXI Mazurian Lakes Conference on Physics, Piaski, Poland, August 30–September 6, 2009.

probe for exploring nuclear structure properties. Indeed, the shell structure, nucleon–nucleon pairing, changes in deformation are directly seen as irregularities on the smooth mass surface [1]. Moreover, it has been shown recently that ground state masses can also contribute to our understanding of excited collective states [2]. Open questions such as the changes of nuclear shell structure, limits of nuclear existence, and new regions of static deformation etc. motivate new experimental and theoretical studies. These investigations involve nuclei with yet unknown masses which lie far away from the valley of β-stability. Such nuclides are characterized by a strong asymmetry of their proton-to-neutron ratio and thus can reveal new nuclear structure properties. It turns out that the masses of these extremely exotic nuclei determine the pathways of nucleosynthesis processes in stars [3]. However, they are difficult to investigate due to their small production cross-sections and short lifetimes and require very efficient and fast experimental techniques. Two such experimental techniques routinely used for direct mass measurements are the Penning trap and storage ring mass spectrometry [4, 5]. These two approaches are highly complementary.

There are several contributions to these proceedings which are devoted to Penning trap mass measurements. Therefore we concentrate here on the storage ring mass spectrometry.

2. Storage ring mass spectrometry

There are presently two facilities worldwide which employ high-energy storage rings for accurate mass measurements. The radioactive beam facility at GSI/Darmstadt is a combination of the high-energy heavy-ion synchrotron SIS [6], the in-flight fragment separator FRS [7], and the cooler-storage ring ESR [8]. The facility is schematically illustrated in Fig. 1. Intense beams of any stable isotope from protons up to uranium can be accelerated by the SIS to a maximum magnetic rigidity of 18 Tm. Relativistic fragments of several hundred MeV/u are produced mainly through fragmentation of primary beam projectiles in thick production targets. In the case of uranium primary beams also the projectile fission is often used for the production of neutron-rich nuclei. Typically beryllium targets with thicknesses of 1–8 g/cm^2 are employed. Secondary beams are separated in flight in the FRS within about 150 ns and are then injected into the ESR [9]. Dependent on the specific experimental requirements, cocktail or clean mono-isotopic beams can be prepared with the FRS by employing magnetic rigidity ($B\rho$) analysis and atomic energy loss (ΔE) in a specially shaped matter [10]. The cocktail beams are ideally used for the mass measurements. Separation of mono-isotopic beams is often essential for accurate lifetime determination [11–15] or reaction studies with the internal target [16].

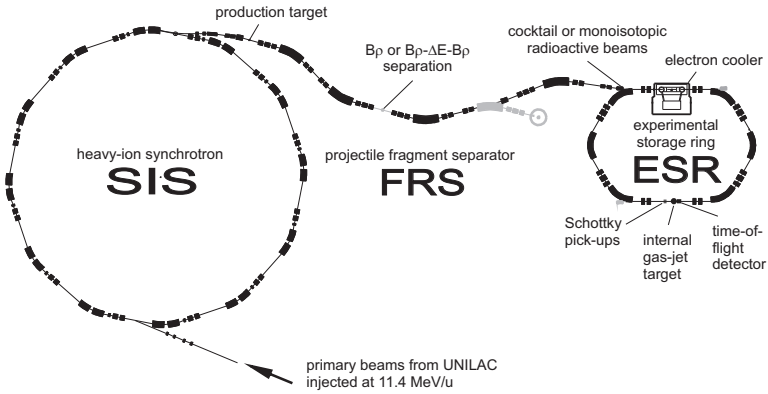

Fig. 1. SIS-FRS-ESR facility at GSI. Primary beams are accelerated in the synchrotron SIS to several hundred MeV/u and impinged on the production target in front of the fragment separator FRS. The reaction products are separated in flight in the FRS and injected into the storage ring ESR for mass measurements [9].

The second storage ring facility has been constructed at IMP/Lanzhou. The high energy part of it is based on the same principle as the one at GSI. It consists of the synchrotron CSRm which is coupled to the storage ring CSRe via the in-flight fragment separator RIBLL2 [17] (see Fig. 2). Some characteristics of the ESR and CSRe rings are summarized in Table I.

TABLE I

Some major parameters of the ESR and CSRe storage rings [8, 17].

	ESR	CSRe
Circumference [m]	108.36	128.80
Maximal magnetic rigidity $B\rho_{\max}$ [Tm]	10.0	8.40
Electron cooling (ion energy) [MeV/u]	4–430	25–400
Stochastic cooling (ion energy) [MeV/u]	400	—
Transition point γ_t (isochronous mode)	1.39–1.41	1.395
Transition point γ_t (standard mode)	2.29	2.629
Acceptance for cooled ions $\Delta(m/q)/(m/q)$	±1.5%	±1.3%

In first-order approximation the revolution frequencies f of the ions stored in the ring can be related to their mass-to-charge ratios (m/q) by the following expression:

$$\frac{\Delta f}{f} = -\frac{1}{\gamma_t^2}\frac{\Delta(m/q)}{(m/q)} + \left(1 - \frac{\gamma^2}{\gamma_t^2}\right)\frac{\Delta v}{v}\,, \tag{1}$$

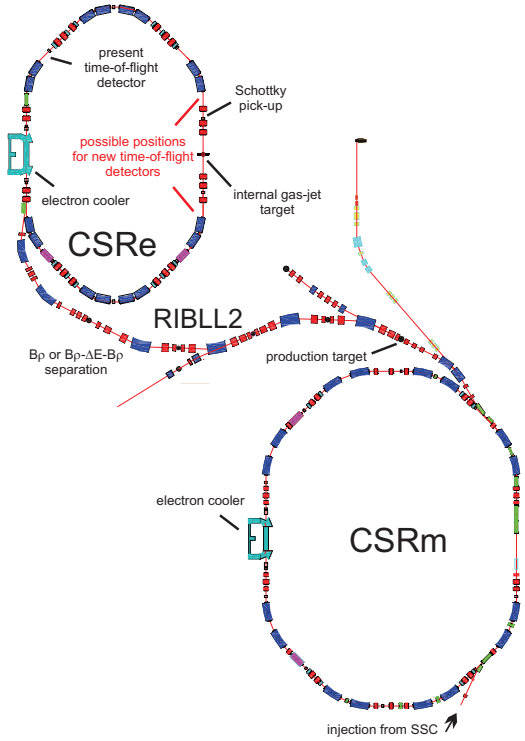

Fig. 2. Schematic view of the radioactive beam facility at IMP/Lanzhou [17]. The synchrotron CSRm accelerates primary beams which are then fragmented in a production target located in front of the in-flight fragment separator RIBLL2. Separated radioactive ions are injected and stored in the storage ring CSRe. Revolution frequencies of the electron-cooled ions can be measured with use of the Schottky pick-up. If the CSRe is tuned into the isochronous ion-optical mode then the revolution frequencies can be obtained also for uncooled particles by using dedicated time-of-flight detectors.

where γ is the relativistic Lorentz factor and γ_t is the transition point of a storage ring [18]. The latter quantity is constant for a given ion-optical setting of the ring. According to the above equation a measurement of the frequencies of the stored ions allows the determination of their m/q values only if the second term on the right-hand side can be neglected. However, secondary beams have a velocity spread $\Delta v/v$ of the order of a few percent which is an inevitable consequence of the nuclear reaction process [10].

Two complementary experimental methods, namely Schottky (SMS) and Isochronous (IMS) Mass Spectrometry, have been developed for accurate mass measurements [5].

In the SMS, the velocity spread can be reduced by stochastic [19] and electron cooling [20], which force all stored ions towards the same mean velocity. A velocity spread of the cooled ions of roughly 5×10^{-7} can be achieved for beam intensities below about a thousand ions [20]. Thus the second term in Eq. (1) can be neglected [21]. The revolution frequencies are measured by the Schottky-noise spectroscopy. The stored ions circulate in the storage ring more than a million times per second. Typical revolution frequencies are about 2 MHz in the ESR and about 1.5 MHz in the CSRe. Each ion induces at each revolution a mirror charge on a couple of electrostatic pick-up electrodes. Fast Fourier transform of these signals yields a spectrum of revolution frequencies. The charges induced on the pick-ups are tiny compared to the thermal noise of the pick-ups and electronics. Therefore, several hundred thousands of revolutions of the ions in the ring are required for producing a frequency spectrum. Locations of the Schottky pick-ups in the ESR and in the CSRe rings are indicated in Figs. 1 and 2, respectively. The disadvantage of the SMS is that the cooling process and spectrum creation last a few seconds. Thus, only nuclides with half-lives longer than about 1 s can be investigated.

Exotic nuclei with half-lives shorter than the cooling time can be studied with a time-of-flight technique by operating the storage ring in the isochronous ion-optical mode. In this case the ions of interest are injected into the ESR or CSRe with $\gamma = \gamma_t \approx 1.41$ or 1.395, respectively. Thus, the term containing the velocity spread in Eq. (1) equals to zero. In this ion-optical mode, a faster ion of a given ion species moves on a longer orbit and a slower ion of the same ion species moves on a shorter orbit, so that the velocity spread is compensated by the lengths of the closed orbits. This means that the revolution frequency of the circulating fragments does not depend on their velocity spread [22,23]. A dedicated time-of-flight detector is used to measure the revolution frequencies [24]. The detector is equipped with a thin (about 10 μg/cm^2) carbon foil. Secondary electrons are released from the foil when it is penetrated by the fast ions. These electrons are guided by the electric and magnetic fields to a set of micro-channel plates. Thus, time stamps of each ion passing at each revolution through the detector are recorded. The fragments do not require cooling and the nuclei with half-lives as short as 10 μs — about 20 revolutions in the ring — can be measured with this method. Present and planned positions of the time-of-flight detectors can be seen in Figs. 1 and 2.

3. Results from Schottky mass spectrometry

SMS is ideally suited for simultaneous mass measurements of a large number of nuclides [21,25,26]. The commissioning of Schottky pick-ups and the corresponding electronics is currently under way at the CSRe. Therefore we restrict ourselves to the experiments performed at the ESR.

The electron cooled ion beams occupy the entire acceptance of the ESR (see Table I). Several ten different nuclides in up to three ionic charge states can be present in one frequency spectrum [26]. An example of a Schottky frequency spectrum is illustrated in Fig. 3. In this experiment ^{238}U projectile

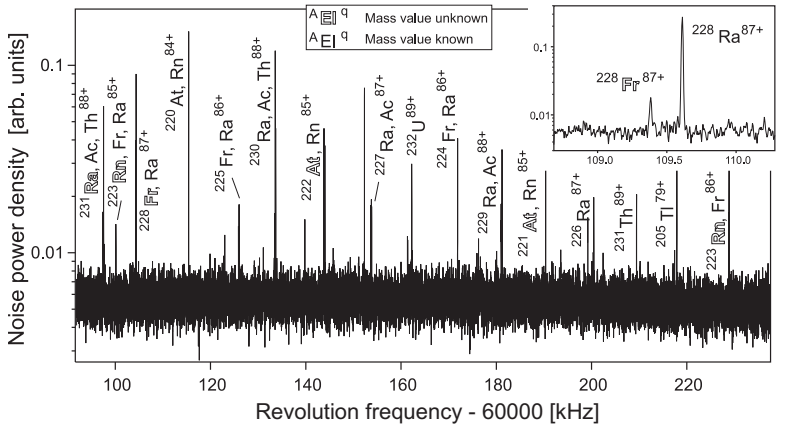

Fig. 3. Schottky frequency spectrum of ^{238}U projectile fragments [29]. Only the prominent peaks are labelled with the corresponding isotope identification. Most of these peaks correspond to isobaric multiplets of the same ionic charge state. This is shown in the inset on the example of the isobaric duplet of ^{228}Ra^{87+} and ^{228}Fr^{87+} ions. There are five nuclides whose masses were not measured before, namely ^{221,222}At, ^{223}Rn, ^{228}Fr and ^{231}Ra. Please note that the ^{223}Rn nuclide is present in two charge states, bare and H-like, at about 230 and 100 kHz, respectively.

fragments have been measured [27–29]. One can see that the nuclides with known and unknown masses are present in this spectrum. The nuclides with known masses are used to calibrate the spectrum by using Eq. (1). The mass values of ^{221,222}At, ^{223}Rn, ^{228}Fr and ^{231}Ra nuclides from this spectrum could be measured for the first time. The ^{223}Rn nucleus is present in two charge states which yields redundant mass determination since in each case it is surrounded by different reference masses. The important achievement of SMS is that the revolution frequency of a single stored ion can be measured [30, 31]. On one side, detecting single ions is of a great advantage for resolving low-lying isomeric states since the ion can only be present in one or the other state [32]. Thus, ground or isomeric states can be assigned even for very small excitation energies which is not possible under the condition when both states are simultaneously populated. One example is illustrated in Fig. 4. In this figure, single ^{125}Ce^{58+} ions have two distinguished revolution frequencies in the upper and lower Schottky spectra. In this way, a long-lived isomeric state in ^{125}Ce with an excitation energy of only $E^* = 103(12)$ keV has been discovered [33]. On the other side,

the nuclides with very small production rates can be measured. Several new isotopes from ^{238}U projectile fragmentation were identified and their masses and half-lives have been measured [29], *e.g.* the ^{235}Ac nuclide [34].

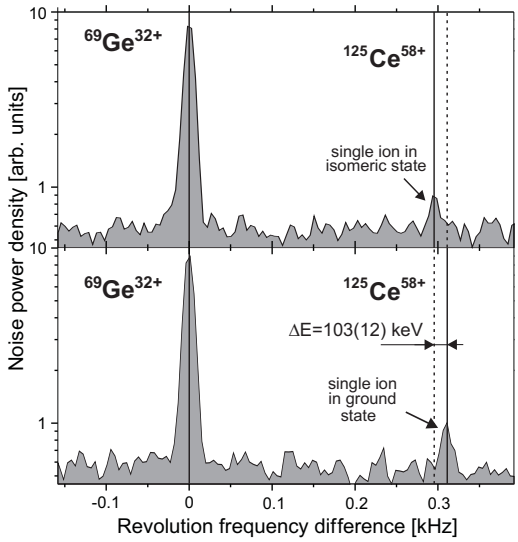

Fig. 4. Schottky frequency spectra of single stored $^{125}Ce^{58+}$ ions in the isomeric (upper spectrum) and in the ground (lower spectrum) state. The measured frequency difference corresponds to the excitation energy of $E^* = 103(12)$ keV. Peaks of $^{69}Ge^{32+}$ are used as a frequency reference.

One important result is for the first time measured mass value of ^{208}Hg ($ME = -13265(31)$ keV) [28]. This mass value has been used to determine the interaction strength of the last two protons with the last two neutrons, commonly denoted as δV_{pn}[1], in ^{210}Pb which amounts to $\delta V_{pn}(^{210}\mathrm{Pb}) = 165.2(10)$ keV. This value is about 2.5 times smaller than the $\delta V_{pn}(^{208}\mathrm{Pb}) = 426.8(5)$ keV. This sudden decrease just after the magic neutron number $N = 126$ (see Fig. 5) confirms the expectations based on the spatial overlap of the valence orbits in this region and their relation to very general properties of the shell structure near stability [28].

The mass surface derived form SMS experiments is illustrated in Fig. 8. The relative mass accuracy of the SMS amounts presently to $\Delta(m)/m \approx 1.5 \times 10^{-7}$. Somewhat better mass accuracy of about $\Delta(m)/m \approx 4 \times 10^{-8}$ can be reached in special cases by using narrow frequency ranges and well known masses for calibration. For example, the mass excess value $ME = -84376(4)$ keV [35] has been obtained for the isomeric state ^{93m}Mo which is

[1] $\delta V_{pn}(Z,N) = 1/4\,[m(Z,N) + m(Z-2,N-2) - m(Z,N-2) - m(Z-2,N)]$, where Z and N are the proton and neutron numbers, respectively.

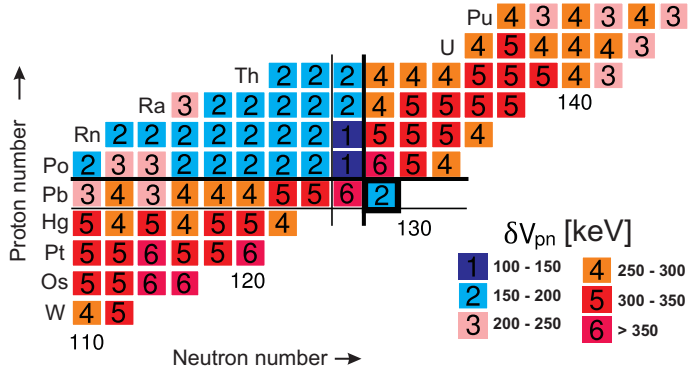

Fig. 5. Experimentally known δV_{pn} values of even–even nuclei on the chart of nuclides. The diagonal symmetry in the δV_{pn} values for lower-left and upper-right quadrants is clearly seen and can be explained by the "symmetry" in the quantum numbers of the single-particle orbitals occupied by the valence nucleons. The newly determined δV_{pn} value for ^{210}Pb is indicated with the black square. Please note that this is the first experimental result for the region $Z \leq 82$ and $N > 126$.

in excellent agreement with the literature value $ME = -84378(4)$ keV [36]. It is important to note that masses of hundreds of nuclei are measured with the same method, that is with the same systematic errors. The obtained mass surface has been successfully used for numerous nuclear structure investigations. Some examples can be found in Refs. [37–41].

4. Results from isochronous mass spectrometry

As discussed above, the SMS can address nuclei with lifetimes longer than about a second. In order to investigate the nuclei with shorter half-lives the IMS is applied. Similarly to SMS, IMS is a broad-band technique. In the case of the ESR, a revolution frequency spectrum covers $\Delta(m/q)/(m/q) \approx 13\%$ [42,43]. The achieved mass resolving powers of IMS are about $m/\Delta m \approx 10^5$ (ESR) and $m/\Delta m \approx 5 \times 10^4$ (CSRe), which has to be compared to $m/\Delta m \approx 10^6$ obtained in SMS experiments. Moreover, for a given $B\rho$, the broad m/q range means that the ions have also a broad range of mean velocities. It turns out that the isochronous conditions, *i.e.* high resolving power, are fulfilled only in a small m/q-range [44].

Left part of Fig. 6 illustrates the variation of the resolving power $\Delta T/T$ as a function of the relative change in magnetic rigidity $\Delta B\rho/B\rho$ for three m/q ratios. It is clear from this figure that the isochronous conditions are fulfilled only for nuclides with m/q close to 2.615. The resolving power can be significantly improved, if an additional measurement of the velocity or magnetic rigidity of each ion is performed [32]. This has been tested at

GSI where in the last experiment addressing ^{238}U fission fragments a new method of $B\rho$-tagging has been employed [44]. The magnetic rigidity has been restricted to about $\Delta(B\rho)/B\rho \approx 1.5\times10^{-4}$. This was done by selecting the particles with a system of asymmetrical slits at the central focal plane of the FRS. In this experiment a mass resolving power of 2×10^5(FWHM) and a typical mass accuracy of 120 keV have been achieved almost over the entire spectrum. The masses of 35 neutron-rich nuclides have been directly measured in the element range from aluminium to barium. The masses of 8 nuclides (^{85,86}As, ^{89}Se, ^{123}Ag, ^{138}Te, ^{140,141}I, ^{143}Xe) have been measured for the first time [45, 46]. Right part of Fig. 6 shows examples of revolution time spectra obtained in the ESR for nuclei far off the optimal isochronous region with (upper panel) and without (lower panel) applying the $B\rho$-tagging method. The new $B\rho$-tagging method is a powerful tool since only a few particles are now sufficient to determine their mass value with a relative accuracy of about $\Delta m/m \approx 2 \times 10^{-6}$. Though the transmission is strongly reduced in this method, the nuclides with production cross-sections in the picobarn range could be accessed [45].

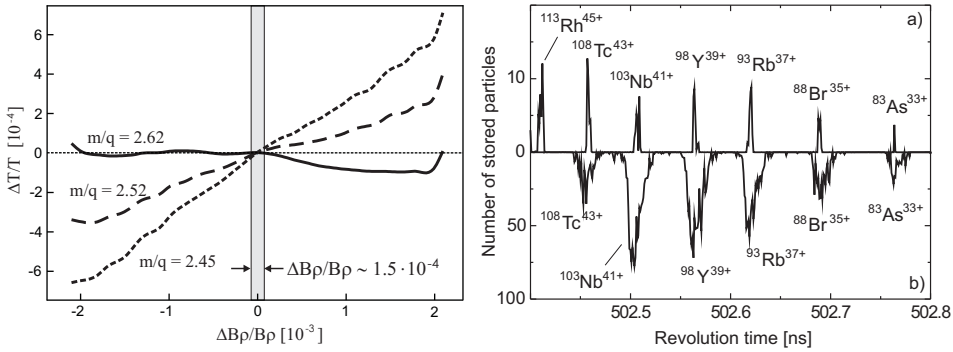

Fig. 6. Left: Resolving power $\Delta T/T$ as a function of the relative change in magnetic rigidity $\Delta B\rho/B\rho$ for three m/q ratios. Right: Measured in the ESR revolution-time spectra. Upper panel: The magnetic rigidity of injected ions has been restricted to $\Delta B\rho/B\rho = 1.5 \times 10^{-4}$ (indicated with grey in the left part). Lower panel: Spectrum measured under nearly identical experimental conditions as in the upper panel except that no restriction in the magnetic rigidities of the ions has been applied.

First IMS experiments have been performed at the CSRe [47, 48]. The masses of ^{63}Ge, ^{65}As and ^{67}Se produced in the fragmentation of ^{76}Kr primary beams have been measured for the first time. The corresponding part of the revolution time spectrum is illustrated in the left part of Fig. 7. The right part shows the comparison of the new masses with the extrapolated values from Ref. [36]. In order to increase the resolving power, the in-

ring velocity measurement of each stored ion is planned. For this purpose, two time-of-flight detectors will be installed in one of the straight sections (see Fig. 2). This velocity measurement will be used to correct for non-isochronous conditions discussed above without restricting the transmission.

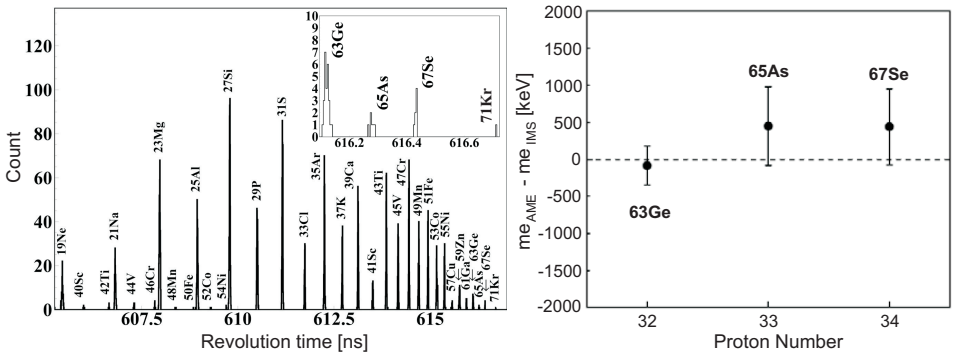

Fig. 7. Left: A revolution frequency spectrum of ^{76}Kr projectile fragments measured in CSRe. Right: Masses of ^{63}Ge, ^{65}As and ^{67}Se have been measured for the first time [48] and are compared to the extrapolated values from Ref. [36]

5. Conclusion and outlook

The mass surface measured with storage ring mass spectrometry covers more that 1000 nuclides and is illustrated in Fig. 8. The sensitivity of both techniques, SMS and IMS, to single stored ions gives access to nuclides with very small production rates. The range of nuclides that can be accessed with the existing GSI and IMP storage ring facilities is indicated with a dotted line in Fig. 8. The new Facility for Antiprotons and Ion Research FAIR will give access to extremely exotic nuclei indicated in this figure with dashed line. Masses and lifetimes of these nuclides will be measured within the NuSTAR/ILIMA-project (Isomeric beams, LIfetimes, and MAsses). The details on the ILIMA project can be found in Refs. [49–52].

The storage ring data contain correlations between masses of *all* nuclides measured in a given experiment (see Fig. 9). One of the future projects is to combine together the correlations from different data sets of IMS and SMS experiments [35]. Thus a global network of correlations between all nuclides ever measured with rings can be established. A single new mass value measured, *e.g.*, with a Penning trap will constrain the entire mass surface via these correlations.

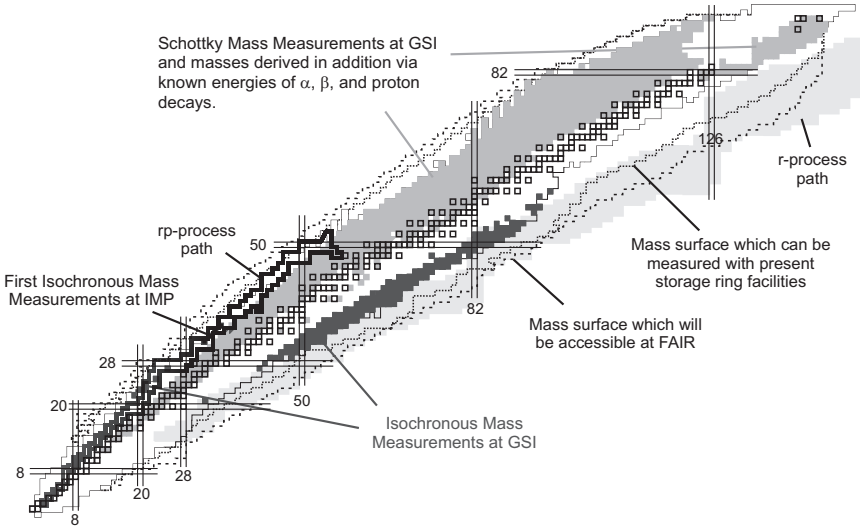

Fig. 8. The mass surface covered with SMS and IMS experiments at GSI (for details see Ref. [41]) and at IMP [47, 48]. The mass surface that can be measured at the present storage ring facilities is shown with the dotted line. The ILIMA project at the future NuSTAR facility at FAIR aims to study nuclei indicated with the dashed line. The r- and rp-process paths of nucleosynthesis are shown as well.

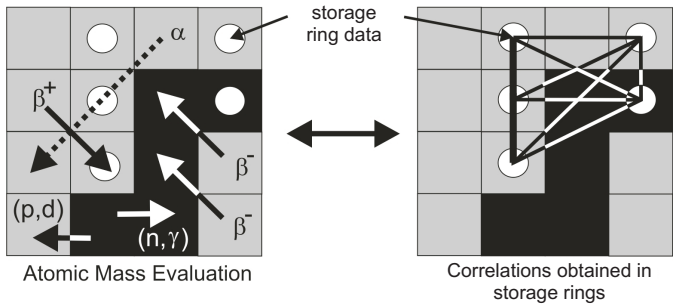

Fig. 9. Schematic view of the AME principle [36] (left) and the correlated data measured with storage ring mass spectrometry (right). In the AME, Q-values from α- and β-decays, reactions (*e.g.*, (n,γ), (p,d) *etc.*) are collected. Every mass value obtained directly (*e.g.* with Penning traps or storage rings) is related to a reference isotope (*e.g.* ^{12}C) and is added as a single relation. The storage ring data provide correlations between all masses measured in a given experiment, and the correlations from different experiments can be combined together [35]. One of the future tasks is to incorporate the measured correlations into the AME.

The authors acknowledge valuable discussions with G. Audi, K. Blaum, F. Bosch, D. Boutin, C. Brandau, B. Cakirli, R. Casten, L. Chen, C. Dimopoulou, B. Franzke, M. Hausmann, C. Kozhuharov, J. Kurcewicz, Z. Liu, X. Ma, G. Münzenberg, F. Nolden, W.R. Plass, C. Scheidenberger, M. Steck, X. Tu, P.M. Walker, M. Wang, H. Weick, N. Winckler, and T. Yamaguchi.

REFERENCES

[1] A. Bohr, B. Mottelson, *Nuclear Structure*, World Scient., Singapore, 1998.
[2] R.B. Cakirli *et al.*, *Phys. Rev. Lett.* **102**, 082501 (2009).
[3] E. Burbidge *et al.*, *Rev. Mod. Phys.* **29**, 547 (1957).
[4] K. Blaum, *Phys. Rep.* **425**, 1 (2006).
[5] B. Franzke, H. Geissel, G. Münzenberg, *Mass Spectrom. Rev.* **27**, 428 (2008).
[6] K. Blasche *et al.*, *IEEE Trans. Nucl. Sci.* **Ns-32**, 2657 (1985).
[7] H. Geissel *et al.*, *Nucl. Instrum. Methods* **B70**, 286 (1992).
[8] B. Franzke, *Nucl. Instrum. Methods* **B24/25**, 18 (1987).
[9] H. Geissel *et al.*, *Phys. Rev. Lett.* **68**, 3412 (1992).
[10] H. Geissel, *Prog. Part. Nucl. Phys.* **42**, 3 (1999).
[11] F. Attallah *et al.*, *Nucl. Phys.* **A701**, 561c (2002).
[12] T. Ohtsubo *et al.*, *Phys. Rev. Lett.* **95**, 052501 (2005).
[13] Yu.A. Litvinov *et al.*, *Phys. Rev. Lett.* **99**, 262501 (2007).
[14] Yu.A. Litvinov *et al.*, *Phys. Lett.* **B664**, 162 (2008).
[15] N. Winckler *et al.*, *Phys. Lett.* **B679**, 36 (2009).
[16] N. Kalantar-Nayestanaki *et al.*, *Int. J. Mod. Phys.* **E18**, 524 (2009).
[17] J.W. Xia *et al.*, *Nucl. Instrum. Methods* **A488**, 11 (2002).
[18] F. Bosch, *Lect. Notes Phys.* **651**, 137 (2004).
[19] F. Nolden, *et al.*, *Nucl. Instrum. Methods* **A532**, 329 (2004).
[20] M. Steck *et al.*, *Nucl. Instrum. Methods* **A532**, 357 (2004).
[21] T. Radon *et al.*, *Nucl. Phys.* **A677**, 75 (2000).
[22] M. Hausmann *et al.*, *Hyperfine Interact.* **132**, 291 (2001).
[23] M. Hausmann *et al.*, *Nucl. Instrum. Methods* **A446**, 569 (2000).
[24] J. Trötscher *et al.*, *Nucl. Instrum. Methods* **B70**, 455 (1992).
[25] Yu.N. Novikov *et al.*, *Nucl. Phys.* **A697**, 92 (2002).
[26] Yu.A. Litvinov *et al.*, *Nucl. Phys.* **A756**, 3 (2005).
[27] Z. Liu, Yu.A. Litvinov, L. Chen, *Int. J. Mod. Phys.* **E15**, 1645 (2006).
[28] L. Chen *et al.*, *Phys. Rev. Lett.* **102**, 122503 (2009).
[29] L. Chen, Ph.D. Thesis, University of Giessen, 2008.
[30] Yu.A. Litvinov *et al.*, *Hyperfine Interact.* **132**, 283 (2001).

[31] H. Geissel *et al.*, *Nucl. Phys.* **A685**, 115c (2001).
[32] H. Geissel, Yu.A. Litvinov, *J. Phys. G* **31**, S1779 (2005).
[33] B. Sun *et al.*, *Eur. Phys. J.* **A31**, 393 (2007).
[34] F. Bosch *et al.*, *Int. J. Mass Spectrom.* **251**, 212 (2006).
[35] Yu.A. Litvinov *et al.*, *Hyperfine Interact.* **173**, 55 (2006).
[36] A. Wapstra, G. Audi, C. Thibault, *Nucl. Phys.* **A729**, 129 (2003).
[37] Yu.A. Litvinov *et al.*, *Nucl. Phys.* **A734**, 473 (2004).
[38] H. Geissel *et al.*, *Nucl. Phys.* **A746**, 150c (2004).
[39] Yu.A. Litvinov *et al.*, *Phys. Rev. Lett.* **95**, 042501 (2005).
[40] Yu.A. Litvinov *et al.*, *Nucl. Phys.* **A787**, 315c (2007).
[41] Yu.A. Litvinov, *Nucl. Phys.* **A805**, 260c (2008).
[42] J. Stadlmann *et al.*, *Phys. Lett.* **B586**, 27 (2004).
[43] B. Sun *et al.*, *Chin. Phys.* **C33**, 161 (2009).
[44] H. Geissel *et al.*, *Hyperfine Interact.* **173**, 49 (2006).
[45] B. Sun *et al.*, *Nucl. Phys.* **A812**, 1 (2008).
[46] B. Sun *et al.*, *Int. J. Mod. Phys.* **E18**, 346 (2009).
[47] X. Tu *et al.*, *Chin. Phys.* **C33**, 516 (2009).
[48] H. Xu *et al.*, *Chin. Sci. Bull.* **54**, 4749 (2009).
[49] C. Scheidenberger *et al.*, *Hyperfine Interact.* **173**, 61 (2006).
[50] H. Geissel, Yu.A. Litvinov, *Nucl. Instrum. Methods* **B266**, 4176 (2008).
[51] H. Weick *et al.*, *AIP Conf. Proc.* **912**, 95 (2007).
[52] Yu.A. Litvinov, *Int. J. Mod. Phys.* **E18**, 323 (2009).